

## Use of relaxation-edited one-dimensional and two dimensional nuclear magnetic resonance spectroscopy to improve detection of small metabolites in blood plasma

Huiru Tang,\* Yulan Wang, Jeremy K. Nicholson, and John C. Lindon

*Biological Chemistry, Biomedical Sciences, Faculty of Medicine, Imperial College London, Sir Alexander Fleming Building, South Kensington, London SW7 2AZ, UK*

Received 24 July 2003

### Abstract

The  $^1\text{H}$  nuclear magnetic resonance (NMR) spectra of biological samples, such as blood plasma and tissues, are information rich but data complex owing to superposition of the resonances from a multitude of different chemical entities in multiple-phase compartments, hampering detection and subsequent resonance assignments. To overcome these problems, several spectral-editing NMR experiments are described here, combining spin-relaxation filters (based on  $T_1$ ,  $T_\rho$ , and  $T_2$ ) with both one-dimensional and two-dimensional (2D) NMR spectroscopy. These techniques enable the separation of NMR resonances based on their relaxation times and allow simplification of the complex spectra. In this paper, the approach is exemplified using a control human blood plasma, which is a complex mixture of proteins, lipoproteins, and small-molecule metabolites. In the case of  $T_{1\rho}$ - and  $T_2$ -edited 2D NMR experiments, a “flip-back” pulse was introduced after the relaxation editing to make the phase cycling of the “relaxation filter” and the 2D NMR part independent, thus enabling easy implementation of the phase-sensitive 2D NMR experiments. These methods also permit much higher receiver gains to be used to reduce digitization error, in particular, for the small resonances, which are sometimes vitally important for metabonomics studies. Both pulse sequences and experimental results are discussed for  $T_1$ -,  $T_{1\rho}$ -, and  $T_2$ -filtered COSY,  $T_2$ -filtered phase-sensitive DQF-COSY, and  $T_1$ ,  $T_{1\rho}$ -, and  $T_2$ -filtered TOCSY NMR.

© 2003 Elsevier Inc. All rights reserved.

**Keywords:** Relaxation-editing; Blood plasma; CPMG; Biofluids; NMR

NMR spectra of biological fluids and intact tissues are rich in useful information. However, they are often complex [1–3] due to the presence of a large number of overlapping resonances from a wide range of molecules [4–6], such as proteins, lipids, lipoproteins, and metabolites, with different line shapes resulting from the biomolecules having a wide range of molecular weights and mobility [4,5]. Consequently, some substances at a low concentration that may be extremely important for classifying toxicological or disease processes are often not observable due to predominating peaks arising from the relatively high concentration of other molecules. In blood plasma, for instance, lipoproteins with intense broad resonances can overwhelm the signals from small

metabolites. In the case of tissues, the dominant lipid resonances sometimes make it prohibitively difficult to observe small metabolite signals [7].

To overcome the above problems and improve the detection, a number of NMR spectral editing methods can be employed utilizing the variation of diffusion properties [8] and spin relaxation [2–5]. Generally, molecules with greater molecular weight diffuse slowly but have relatively short spin-relaxation times, whereas small molecules diffuse quickly but have relatively long spin-relaxation times (unless they are bound to macromolecules). Therefore, the complex NMR spectra of biofluids can be edited by taking advantage of the differences in diffusivity and spin-relaxation times.

Diffusion-edited NMR spectroscopy has been implemented by inserting a “diffusion filter” to eliminate resonances from the fast-diffusing molecules [8–11] prior

\* Corresponding author. Fax: +44-20-7594-3226.

E-mail address: [huiru.tang@imperial.ac.uk](mailto:huiru.tang@imperial.ac.uk) (H. Tang).

to the detection. Both 1D<sup>1</sup> and 2D diffusion-edited NMR methods have been reported for the study of biofluids to aid the assignment of resonances arising from lipoproteins [8,10,11], nucleotides [12], and amino acid mixtures [13].

For spin-relaxation editing, a “relaxation filter” can be inserted in a similar fashion, prior to detection, to attenuate or eliminate the resonances having relatively short relaxation times. Three major spin-relaxation phenomena can be encountered, spin–lattice relaxation characterized by  $T_1$  and  $T_{1\rho}$  and spin–spin relaxation described by  $T_2$ . All these editing methods have been widely used in high-resolution NMR of biopolymers in the solid state [14–19] for many years and have proven useful. While the three relaxation times are identical for small molecules tumbling rapidly and isotropically, they can be different in multiphase, multi-compartment systems, such as biofluids and tissues.

To use  $T_1$ -editing, an inversion-recovery sequence ( $180^\circ_x - \tau_1 - 90^\circ_x$ ) can be employed to prepare spins in such a way that NMR signals in the final spectrum have intensities depending upon the length of  $\tau_1$  relative to  $T_1$ . The  $90^\circ$  pulse can serve as a read-pulse in 1D experiments or the excitation pulse for 2D experiments. One can conveniently make a choice of  $\tau_1$  to have a positive peak ( $\tau_1 > T_1 \ln 2$ ), negative peak ( $\tau_1 < T_1 \ln 2$ ), or no peak at all ( $\tau_1 = T_1 \ln 2$ ). The  $T_1$ -editing has been reported as WEFT in 1D NMR as a method of solvent suppression [20].

Similarly, the magnetization can be prepared using a spin-locking sequence ( $90^\circ_x - \tau_{\text{SPY}}$ ) such that resonances with different  $T_{1\rho}$  can be separated by choosing an appropriate spin-lock time,  $\tau_{\text{SP}}$ , and spin-lock power. So far, there are no reported results on  $T_{1\rho}$ -edited NMR spectroscopy of biofluids and tissues.

In the case of  $T_2$ -editing, the magnetization can be prepared using a spin-echo sequence, typically a CPMG sequence, ( $90^\circ_x - (\tau_E - 180^\circ_y - \tau_E)_n$ ), by choosing  $\tau_E$  and  $n$  such that signals can be separated according to their  $T_2$  (i.e., inverse of the line width). Generally, the broad NMR signals from macromolecules or bound small molecules are attenuated or even eliminated, leaving the sharper resonances from the mobile small molecules unaffected. The resonances having intermediate  $T_2$  will be attenuated to an intermediate extent.  $T_2$ -edited 1D NMR spectroscopy has been employed in solvent suppression [21] and has become a standard method in biofluids studies.

However, the  $T_1$ -,  $T_{1\rho}$ -, and  $T_2$ -edited 1D NMR spectra of biological samples can still be complex since NMR spectral peaks from the low concentration metabolites can still be severely overshadowed. Consequently, it is necessary to extend the relaxation editing approach to multidimensional NMR spectra to establish

atomic connectivity and to achieve resonance assignments unambiguously. Examples for  $T_1$ - and  $T_2$ -edited COSY NMR methods have been reported in studying biological tissues [22,23]. The  $T_2$ -edited 2D COSY [21] and 2D J-resolved NMR [24] methods have also been used to suppress water (known as WATR) so as to characterize the solutes.  $T_2$ -edited 1D NMR has been extensively employed in plasma studies and most of the early work was reviewed [25] systematically in 1988. Recently, an example of the  $T_2$ -filtered TOCSY method was employed for the study of pig blood plasma [26]. All these reported  $T_2$ -filtered 2D NMR methods appear to be a direct attachment of COSY or TOCSY sequences to the relaxation filters and no experimental information was given, in particular, for the phase-sensitive experiments. While such a direct attachment is suitable for the phase-insensitive COSY, J-resolved, and  $T_1$ -edited 2D NMR experiments, it is nontrivial to implement the  $T_{1\rho}$ - and  $T_2$ -edited phase-sensitive experiments such as TOCSY and DQF-COSY.

In effect, TOCSY and ROESY experiments can be considered “mild”  $T_{1\rho}$ -edited methods since  $T_{1\rho}$  relaxation occurs during the mixing time (spin-lock). J-resolved 2D NMR experiment can also be regarded a  $T_2$ -edited experiment. However, in all these cases, the relaxation editing is restricted by the needs of 2D (e.g., TOCSY, ROESY, and J-resolved) NMR experiments. Therefore, explicit relaxation editing sequence is often essential.

In this paper, we extend the concept of relaxation editing to  $T_{1\rho}$ -edited 1D NMR and  $T_1$ -,  $T_{1\rho}$ -, and  $T_2$ -edited 2D experiments, in particular, the phase-sensitive experiments, such as  $T_2$ -edited phase-sensitive DQF-COSY and  $T_1/T_{1\rho}/T_2$ -edited TOCSY. These methods were tested with a control human blood plasma sample. A “flip-back” pulse is introduced immediately after the  $T_{1\rho}$ - and  $T_2$ -editing, making it easier to implement the edited 2D experiments, in particular, the phase-sensitive ones such as DQF-COSY and TOCSY.

## Materials and methods

### Sample preparation

A control blood plasma sample was prepared using standard methods from a local healthy volunteer. The sample was diluted with an equal volume of isotonic saline solution (pH 7.4) containing 10%  $D_2O$  for the NMR field lock; 600  $\mu\text{L}$  of the prepared sample was transferred into a 5-mm NMR tube for measurements.

### Pulse sequences

Figs. 1A–C show the relaxation “filters” for  $T_1$ ,  $T_2$ , and  $T_{1\rho}$ . In the  $T_1$  filter (Fig. 1A), a standard

<sup>1</sup> Abbreviations used: 1D, one-dimensional; 2D, two-dimensional; TSP, trimethylsilyl propionic acid.

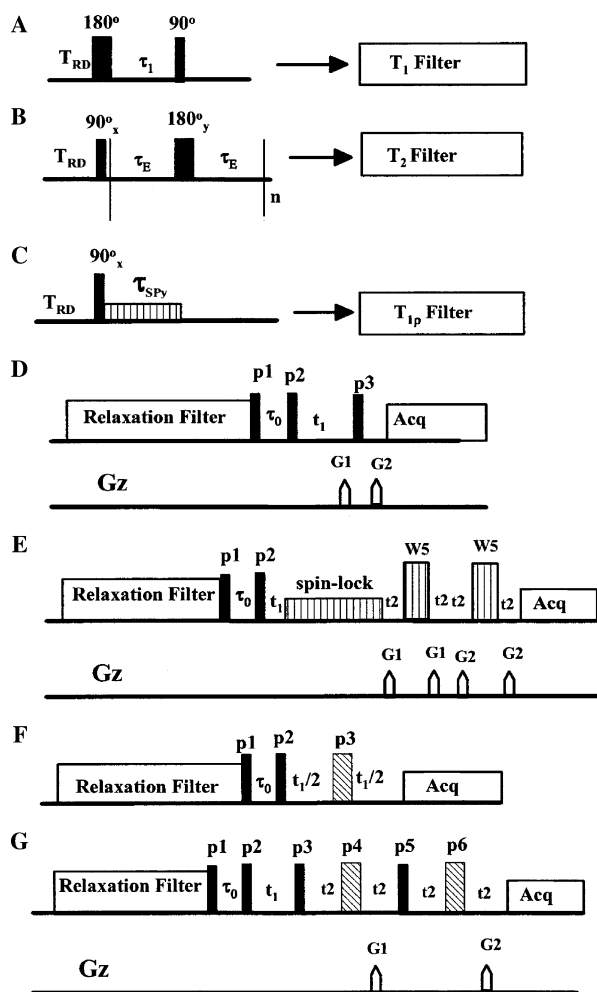


Fig. 1. Pulse sequences for relaxation-edited NMR spectroscopy. (A) A  $T_1$  (inversion-recovery) filter which can be followed with direct acquisition or 2D sequences; phase cycling for  $180^\circ$  pulse,  $+x, -x$ ; for  $90^\circ$  pulse, the same phase cycling as the first pulse of the 2D sequences or  $+x, +x, -x, -x, +y, +y, -y, -y$  in the case of 1D. (B) A  $T_2$  (CPMG) filter; phase cycling for  $90^\circ$  pulse,  $+x, +x, -x, -x, +y, +y, -y, -y$ ; for  $180^\circ$  pulse,  $+y, -y, +y, -y, +x, -x$ . (C)  $T_{1\rho}$  (spin-lock) filter which can be followed with direct acquisition or 2D sequences; phase cycling for  $90^\circ$  pulse,  $+x, -x, +y, -y$ ; for spin-lock pulse,  $+y, -y, -x, +x$ . (D) Relaxation-edited COSY with gradient selection, where p1 is a “flip-back” pulse; phase cycling for p1,  $T_2$ -edited version,  $-x, -x, +x, +x, -y, -y, +y, +y$ ;  $T_{1\rho}$ -edited version,  $-x, +x, -y, +y$ ; normal phase cycling is used for the COSY [36]. (E) Relaxation-edited TOCSY with gradient selection and WATERGATE (W5) [37] as water suppression, where p1 is a “flip-back” pulse, p2 is a  $90^\circ$  pulse, and the usual phase increment schemes (e.g., TPPI) can apply; phase cycling for p1,  $T_2$ -edited version,  $-x, -x, +x, +x, -y, -y, +y, +y$ ;  $T_{1\rho}$ -edited version,  $-x, +x, -y, +y$ ; phase cycling for p2 is the same as the normal one for the unedited TOCSY [36]. (F) Relaxation-edited J-resolved sequence, where p1 is a “flip-back” pulse, p2 a  $90^\circ$  pulse, and p3 an  $180^\circ$  pulse; phase cycling for p1,  $T_2$ -edited version,  $-x, -x, +x, +x, -y, -y, +y, +y$ ;  $T_{1\rho}$ -edited version,  $-x, +x, -y, +y$ ; p2 and p3 have the same phase cycling scheme as in the normal J-resolved. (G) Relaxation-edited phase-sensitive DQF-COSY, where p1 is a “flip-back” pulse, p2, p3, and p5 are  $90^\circ$  pulses, p4 and p6 are  $180^\circ$  pulses, and  $t_1$  is the evolution period; phase cycling for p1,  $T_2$ -edited version,  $-x, -x, +x, +x, -y, -y, +y, +y$ ;  $T_{1\rho}$ -edited version,  $-x, +x, -y, +y$ ; p2, p3, p4, p5, and p6 have the same phase cycling scheme as in the normal DQF-COSY [36]; for  $T_1$ -edited, p1,  $\tau_0$  and  $90^\circ$  pulse of the “filter” are not needed.

inversion-recovery sequence is employed and the relaxation delay,  $\tau_1$ , can be adjusted so that the edited resonances can be recorded before or after the magnetization vectors have passed through the  $x$ - $y$  plane. Alternatively the signals can be zeroed. In a  $T_2$  filter (Fig. 1B), a standard CPMG sequence is used as reported previously [27], where both  $\tau_E$  and  $n$  can be adjusted. However,  $\tau_E$  has to be short (250–400  $\mu$ s) compared to the inverse of any spin-spin couplings to avoid J-modulation. In a  $T_{1\rho}$  filter (Fig. 1C), both the length and the power of the spin-lock can be adjusted to edit out the short  $T_{1\rho}$  components.

Fig. 1D shows the sequence for the relaxation-edited  $^1\text{H}$ - $^1\text{H}$  2D COSY NMR. In the case of  $T_2$ -editing, it differs from that reported previously [22] in which the COSY sequence was simply attached to the CPMG part. In this implementation, a  $90^\circ$  pulse, p1, is introduced as a “flip-back” pulse, returning the prepared net transverse magnetization to the  $z$  axis and storing it for a short period of 2–3  $\mu$ s, during which the relaxation is negligible. In the case of  $T_1$ -editing, both the flip-back pulse and the p2 are not needed since the prepared net-magnetization lies in the  $z$  axis. Full phase cycling is necessary for p1 to minimize any artifacts. The pulses p2 and p3 can be implemented in the same way as that in the normal COSY (p2,  $90^\circ$ ; p3,  $20$ – $90^\circ$ ) [28] including the phase cycling schemes. The flip-back pulse makes it simple to implement phase-sensitive experiments, e.g., the phase increment of p2, and the phase cycling schemes for the relaxation filter and COSY become independent of each other. The full phase cycling (Fig. 1) is necessary for both the CPMG and the flip-back pulse to minimize artifacts. This approach was, in particular, tested for a phase-sensitive  $T_2$ -edited DQF-COSY experiment (Fig. 1G). The sequences for  $T_1/T_{1\rho}/T_2$ -edited TOCSY and J-resolved NMR methods are shown in Figs. 1E and F, respectively, where the signals were selectively emphasized according to their relaxation times. In principle, other 2D NMR, such as ROESY, can be implemented in a similar fashion.

### NMR measurements

All the NMR experiments were carried out without spinning at 600.22 MHz on a Bruker DRX600 spectrometer (Bruker Biospin, Rheinstetten Germany) equipped with a 5-mm inverse-broad-band probe. The chemical shift was referenced to that of the lactate doublet (at 1.33 ppm relative to TSP) since TSP is not a suitable reference in the plasma samples due to interaction-induced line broadening.

All 1D  $^1\text{H}$  NMR spectra were acquired with a spectral width of 7.2 kHz, at 300 K, into 32 K data points zero-filled to 64 K before Fourier transformation. The other parameters were recycle delay 2 s, 64 scans, 8 dummy scans, and  $90^\circ$  pulse length about 10  $\mu$ s.

1D NOESYPR1D spectra were recorded with the standard sequence  $90^\circ_x-t_0-90^\circ_x-t_m-90^\circ$ -Acq [29]. Water presaturation was achieved by selective irradiation of water signal with a power equivalent to 50 Hz during the mixing time ( $t_m$ ) of 150 ms and during the recycle delay of 2 s unless stated otherwise. The delay between the first two  $90^\circ$  pulses ( $t_0$ ) was 3  $\mu$ s. The  $T_1$ -edited 1D  $^1\text{H}$  NMR spectrum was recorded using the sequence shown in Fig. 1A with  $\tau_1$  of 0.265 s and a total repetition time (recycle delay plus acquisition time) of 10 s. The  $T_2$ -edited 1D  $^1\text{H}$  NMR spectrum was recorded using the sequence shown in Fig. 1B with  $\tau_E$  of 400  $\mu$ s and 400 loops (**n**). The  $T_{1\rho}$ -edited 1D  $^1\text{H}$  NMR spectrum was recorded using sequence shown in Fig. 1C with  $\tau_{SP}$  of 120 ms and spin-lock power equivalent to 5 kHz.

$^1\text{H}$   $T_1$  was measured using a standard inversion-recovery pulse sequence ( $180^\circ_x-\tau_1-90^\circ_x$ ). Sixteen spectra were acquired with the same acquisition parameters as in the 1D NMR described above except for recycle delay, which was 12 s. The relaxation delay,  $\tau_1$ , was chosen logarithmically as described previously [30–35], to cover the values of 0.05–12 s.

$^1\text{H}$   $T_{1\rho}$  was measured using a standard spin-lock pulse sequence ( $90^\circ_x-\tau_{SP}$ ). The spin-lock power was adjusted to be equivalent to 5 kHz and the spin-lock time (relaxation delay),  $\tau_{SP}$ , was chosen in the same logarithmic fashion [30–35] as in the  $T_1$  measurement to cover the values of 5–200 ms.  $T_{1\rho}$  with values greater than 200 ms was not possible to measure with this method since long spin-lock time (>200 ms) was not permitted for the safety of probe head and samples. The  $T_{1\rho}$  can be measured at a lower spin-lock power. Sixteen spectra were acquired with the same acquisition parameters as those in the 1D NMR described above except for recycle delay, which was 12 s.

$T_2$  was measured using a standard CPMG approach. Sixteen relaxation delays (800  $\mu$ s–9.6 s) were chosen logarithmically as described previously [30–35] to enable easy detection of multiple processes. The  $T_2$  values were extracted from fitting the intensity of a given signal as a function of relaxation delays assuming single or biexponential decay processes as appropriate. The effective relaxation times,  $T_2^*$ , of lactate (1.33 ppm) and glucose (4.65 ppm, 5.23 ppm) were also estimated from the line width assuming Lorenz line shapes.

The 2D NMR spectra were acquired into 2K data points for the acquisition dimension ( $f_2$ ) and 128 increments for the indirect dimension ( $f_1$ ) except for the J-resolved spectrum, which was recorded with 48 increments. The time domain data were Fourier transformed into  $2\text{K} \times 2\text{K}$  points except for the J-resolved spectrum, which was transformed into 128 points for the second dimension.

Relaxation-edited 2D COSY spectra were recorded with gradient selection (Fig. 1D) with water presaturation. The  $T_2$ -filtered phase-sensitive DQF-COSY spec-

trum was also recorded with gradient selection [36] (Fig. 1G). For the  $T_{1\rho}$ - and  $T_2$ -filtered TOCSY experiments, gradient selection was also employed and the water suppression was achieved with an improved version of WATERGATE [37]. For the phase-sensitive 2D experiments, the phase increment in the second dimension was implemented according to the TPPI scheme [38] following a “flip-back” pulse, p1 (Fig. 1). For other “phase-insensitive” experiments, the flip-back pulse is optional. For the  $T_1$ -filtered experiments, the flip-back pulse was not inserted. For the  $T_{1\rho}$ -edited TOCSY, two methods were tested using a “ $T_{1\rho}$  filter” as shown in Fig. 1E and prolonged mixing time. For  $T_2$ -filtered TOCSY, both MLEV-17 [39] and DIPSI2 [40] sequences were tested for the spin-lock schemes. The  $T_2$ -edited 2D J-resolved spectrum was recorded with the sequence initially proposed by Rabenstein et al. [24].

## Results and discussion

### 1D $^1\text{H}$ $T_1/T_{1\rho}/T_2$ -filtered NMR spectroscopy of human blood plasma

Fig. 2 shows 1D  $^1\text{H}$  NMR spectra of a typical control human blood plasma sample; Fig. 2A shows a normal  $^1\text{H}$  NMR spectrum, obtained using the NOESYPR1D pulse sequence. This spectrum contains effectively all  $^1\text{H}$  resonances in the sample although their relaxation properties are drastically different. The  $T_1$ ,  $T_{1\rho}$ , and  $T_2$  values of these peaks have been measured;  $T_2$  values of resonances at 1.33 ppm (lactate), 4.65 ppm ( $\beta$ -glucose), and 5.23 ppm ( $\alpha$ -glucose) were also estimated from their line widths. Some of the  $T_1$  and  $T_{1\rho}$  data are shown in Table 1. It is clear that the  $T_1$  values of the protons in the small metabolites (showing sharp resonances) are about 1–2.5 s while these of the lipid protons of lipoproteins (showing broad peaks) are much smaller, being in accord with observations reported previously [11]. The  $T_1$  values are in fact about 0.3–0.4 s for the proteins/lipoproteins.

In dilute solution, the values of  $T_{1\rho}$  and  $T_2$  of the small metabolites, such as amino acids and glucose, are expected to be identical to their  $T_1$  values due to fast isotropic motions ( $\omega_0^2\tau_c^2 \ll 1$ ). However, in a system as complex as blood plasma, the situation can be different. For example, the measured  $T_2$  values (Table 1) were about 280, 260, and 160 ms, respectively, for H-1 of  $\alpha$ -glucose (5.23 ppm), H-1 of  $\beta$ -glucose (4.65 ppm), and lactate (1.33 ppm). The value for lactate is, in fact shorter than  $T_2^*$  ( $\Delta\nu_{1/2} \sim 1.5$  Hz). The poor accuracy of  $T_2$  measurements for the sharp metabolite peaks is probably due to severe overlapping with the broad protein/lipid signals. So far, there are no improved methods reported to deal with this problem. Multiple-component relaxation has also been detected for the broad peaks. For

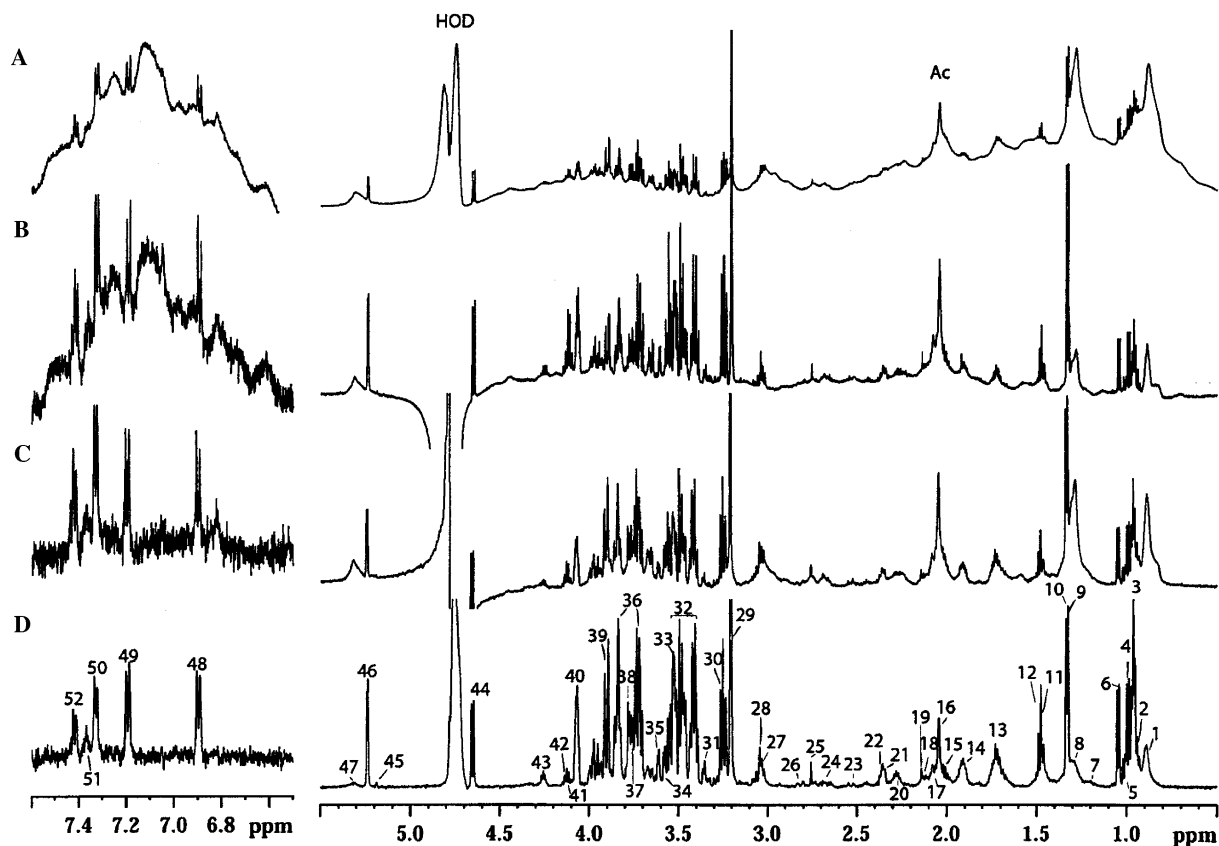


Fig. 2. 1D  $^1\text{H}$  NMR spectra of a human blood plasma sample, (A) NOESYPR1D with water presaturation; (B)  $T_1$ -edited NMR spectrum plotted inverted (with  $180^\circ$  phase shift);  $\tau_1 = 0.265$  s; (C)  $T_{1\rho}$ -edited NMR spectrum; spin-locking time, 120 ms; spin-locking power, 5 kHz; (D)  $T_2$ -edited NMR spectroscopy; spin echo delay, 400  $\mu\text{s}$ ; loop-number, 400. Resonance assignments are given in Table 2.

example, the resonances at 7.72, 7.06, and 6.86 ppm, assigned to proteins, showed  $T_2$  values of 4–9 ms; the peak at 0.89 ppm, corresponding to  $\text{CH}_3$  of lipids, showed two  $T_2$  components of 7 and 90 ms; the peaks at 1.278 and 1.296 ppm ( $\text{CH}_2$  of lipids) also showed two  $T_2$  components of 7 and 70–90 ms, respectively. Their exact structural characteristics are unknown at present but they can be tentatively assigned to proteins/lipoproteins ( $<10$  ms) and more mobile lipids (70–90 ms). For the purpose of spectral editing in this work, it is interesting to note that the  $T_2$  of lipoproteins and proteins ( $\sim 10$  ms) is more than an order of magnitude shorter than the  $T_2$  of the metabolites ( $>100$  ms). Even for the intermediate  $T_2$  component, its  $T_2$  (70–90 ms) is much shorter than that of the metabolites. These differences in the  $T_2$  relaxation times of macromolecules and a small metabolites provide a good basis for spectral editing.

In the case of  $T_{1\rho}$ , the values are 10–50 ms for proteins/lipoproteins (Table 1), which are about an order of magnitude smaller than the corresponding  $T_1$  values (0.3–0.5 s). This implies that the proteins/lipoproteins are “rigid” as far as  $T_1$  is concerned ( $\omega_0^2\tau_c^2 \gg 1$ ) but are still in the extreme narrowing situation [41] for  $T_{1\rho}$  ( $\omega_{\text{SP}}^2\tau_c^2 \ll 1$ , where  $\omega_{\text{SP}}$  is the spin-lock field in frequency

units). The  $T_{1\rho}$  values for small metabolites were too long to be measured with reasonable accuracy even with relaxation delays as long as 200 ms. It is, thus, reasonable to assume that their  $T_{1\rho}$  values are longer than 200 ms. Therefore,  $T_{1\rho}$  for small metabolites is also about an order of magnitude longer than that for proteins/lipoproteins, offering great opportunities for  $T_{1\rho}$ -based spectral editing. In a multiphase, multicompartiment system, such as blood plasma and semi-solid biological samples, more than one component may exist for  $T_1$ ,  $T_{1\rho}$ , and  $T_2$  relaxation processes. Nevertheless, the differences in the  $T_1$ ,  $T_{1\rho}$ , and  $T_2$  relaxation times of different chemical moieties can be exploited for the purpose of spectral editing.

Fig. 2B shows a 1D  $T_1$ -edited NMR spectrum of human blood plasma using a relaxation delay of 0.265 s. At this point, the resonances with  $T_1$  longer than 0.382 s ( $0.265/\ln 2$ ) are still inverted and for the convenience of plotting, the spectrum was  $180^\circ$  phase-shifted. Compared with the unedited 1D spectrum (Fig. 2A), the broad signals at 0.8–0.9, 1.2–1.4, 1.5, 1.9–2.1, 2.7–3.0, 5.1–5.4, and 6.5–8.0 ppm, corresponding to signals of lipoproteins and proteins, have been substantially attenuated or almost zeroed, whereas the sharp resonances

Table 1  
Spin relaxation times for some resonances of human blood plasma

$\delta$ (ppm)	$T_1$ (s)	$T_{1\rho}$ (ms) <sup>a</sup>	$T_2$ (ms)	Assignment
7.72	0.35 (estimated)	28 ± 10	4.98 ± 0.93	Protein (broad)
7.43	1.1 (estimated)	<sup>b</sup>	—	Phenylalanine
7.34		<sup>b</sup>	—	
7.06	0.35 (estimated)	25 ± 7	6.96 ± 0.67	Protein (broad)
7.18	1.1 (estimated)	<sup>b</sup>	—	Tyrosine
6.89		<sup>b</sup>	—	
6.86	0.35 (estimated)	35 ± 10	8.74 ± 0.66	Protein (broad)
5.32	0.43 ± 0.08	39 ± 13	16.00 ± 4.39	Lipids (CH=CH)
5.23	2.29 ± 0.14	<sup>b</sup>	280 ± 21 <sup>c</sup>	$\alpha$ -Glucose
		—	17.12 ± 2.76 <sup>c</sup>	Broad peak underneath
4.65	2.14 ± 0.12	—	257 ± 39 <sup>c</sup>	$\beta$ -Glucose
		—	7.79 ± 1.67 <sup>c</sup>	Broad peak underneath
3.21	2.41 ± 0.12	<sup>b</sup>	165 ± 5 <sup>c</sup>	N(CH <sub>3</sub> ) <sub>3</sub> , choline
	0.33 ± 0.02	23 ± 4	4.18 ± 0.57 <sup>c</sup>	Lipoproteins
2.04	1.06 ± 0.03	<sup>b</sup>	84.6 ± 12.4 <sup>c</sup>	Acetate
	0.36 ± 0.02	14 ± 6	4.71 ± 0.65 <sup>c</sup>	Lipoproteins
1.48	1.4 (estimated)	<sup>b</sup>	63 ± 29 <sup>c</sup>	Alanine
		—	4.61 ± 1.67 <sup>c</sup>	Broad peak underneath
1.33	1.59 ± 0.12	—	161 ± 38 <sup>c</sup>	Lactate
	0.30 ± 0.02	53 ± 15	5.71 ± 1.86 <sup>c</sup>	Lipids (–CH <sub>2</sub> –)/lipoproteins
1.296	0.40 ± 0.02	60 ± 8	6.19 ± 1.09 <sup>c</sup>	Lipids (–CH <sub>2</sub> –)/lipoproteins
			74 ± 10 <sup>c</sup>	Mobile lipids
1.278	0.35 (estimated)	30 ± 8	7.60 ± 0.64 <sup>c</sup>	Lipids (–CH <sub>2</sub> –)/lipoproteins
			78 ± 5 <sup>c</sup>	Mobile lipids
1.04	1.4 (estimated)	<sup>b</sup>	93 ± 32 <sup>c</sup>	Valine
		—	5.19 ± 0.44 <sup>c</sup>	Broad peak underneath
0.99	1.4 (estimated)	<sup>b</sup>	—	Valine
0.89	0.38 ± 0.02	50 ± 6	7.27 ± 1.02 <sup>c</sup>	Lipids (–CH <sub>3</sub> )/lipoproteins
			90 ± 16 <sup>c</sup>	Mobile lipids

<sup>a</sup> The measured  $T_{1\rho}$  values are for the broad resonance.

<sup>b</sup>  $T_{1\rho}$  for the sharp resonances cannot be measured with the short relaxation delays (up to 200 ms) used in the experiments due to limited decay of signal intensity. This implies much longer  $T_{1\rho}$  for them compared to 200 ms.

<sup>c</sup> Bi-exponential decay was observed and evaluated.

of small metabolites remain inverted (Fig. 2B; bearing in mind that the spectrum was 180° phase-shifted). Assuming exponential  $T_1$  relaxation processes for the small metabolites protons, there ought to be some signal intensity loss for the small metabolites (due to relaxation) on the order of 20% during the relaxation delay (0.265 s). Nevertheless, the removal of the intense broad signals enables the metabolite signals to be more easily observed and allows increased receiver gain (~15-fold) to be used to reduce the digitization errors, favoring the detection of small metabolite signals.

In the case of the  $T_{1\rho}$ -edited spectrum with a relaxation time of 120 ms (Fig. 2C), similar effects were brought about although the intensity of the broad peaks was evidently attenuated to a lesser degree than that of the  $T_1$ -edited spectrum. With the  $T_{1\rho}$  values of proteins and lipoproteins on the order of 15–60 ms and the relaxation period of 120 ms, the protein/lipoprotein signals were attenuated substantially (86–98%). However, the sharp signals suffered less intensity reduction, based on the assumption that all the  $T_{1\rho}$  processes were exponential and  $T_{1\rho}$  values for the metabolites were greater than these for proteins/lipoproteins. The attenuation

sufficed to reveal the “buried” sharp signals such as methyl resonances of isoleucine (0.94–1.01 ppm)/leucine (0.97 ppm), glutamine (2.12, 2.44 ppm), and glutamate (2.08, 2.35 ppm). This technique again allowed increased receiver gain (up to fivefold) to be used to enhance the detection of the small signals.

A  $T_2$ -edited spectrum (Fig. 2D), using a total relaxation delay of 320 ms, showed that the broad resonances from proteins and lipoproteins are almost completely attenuated, leaving most of the sharp resonances observable although their intensity suffered some loss also. This experiment is well known and has been used extensively [2–5]. To maximize the differentiation in this experiment, a much longer relaxation filter was applied than that employed in the literature [4] (~90 ms). On the other hand, even with such a long relaxation delay, some lipid signals (**1**, **2**, **8**, **47**) are still visible due to their long  $T_2$  (about 70–90 ms). There are clear similarities between the effects of  $T_{1\rho}$ -editing and  $T_2$ -editing for this particular sample since the  $T_{1\rho}$  differences between small metabolites and proteins/lipoproteins were similar to the  $T_2$  differences between them. However, in semisolid systems, such as tissues, where  $T_{1\rho}$  and  $T_2$  values are

markedly different, both methods should be independently useful. Nevertheless, in the  $T_2$ -editing, long relaxation periods can be tolerated without concern over sample heating caused by the spin-lock in the  $T_{1\rho}$  experiments. Compared to  $T_{1\rho}$ - and  $T_2$ -edited spectra, the  $T_1$ -edited spectrum (Fig. 2B) showed relatively more intense signals for lactate (**10**, **42**) and threonine (**43**).

The intensity of lipid resonances (**1**, **8**, and **47**) in the  $T_1$ -edited spectrum is only slightly higher than that in the  $T_2$ -edited spectrum but much lower than that in  $T_{1\rho}$ -edited one. Therefore,  $T_1$ -editing is particularly efficient in distinguishing two groups of signals.

Most of the sharp peaks are readily assigned according to the literature [4] (Table 2). A number of

Table 2

$^1\text{H}$  NMR assignment for human blood plasma as detailed in the figure captions

Peak	$\delta$ (ppm)	Coupling pattern (Hz)	Assignments
1	0.89	br	Lipid, $\text{CH}_3\text{CH}_2\text{CH}_2\text{C}=\text{}$
2	0.94	d(7.6)	Isoleucine, $\delta\text{-CH}_3$
3	0.97	t(6)	Leucine, $\delta\text{-CH}_3$
4	0.99	d(7.0)	Valine $\text{CH}_3$
5	1.01	d(7.0)	Isoleucine $\beta\text{-CH}_3$
6	1.04	d(7.0)	Valine, $\text{CH}_3$
7	1.20	d(6)	3-hydroxybutyrate $\gamma\text{-CH}_3$
8	1.29	br	Lipid, $\text{CH}_2\text{CH}_2\text{CH}=\text{CH}$
9	1.32	d(6.5)	Threonine, $\gamma\text{-CH}_3$
10	1.33	d(6.6)	Lactate
11	1.47	m	Lysine $\delta\text{-H}$
12	1.48	d(7.0)	Alanine $\text{CH}_3$
13	1.72	m	Arginine ( $\gamma\text{-H}$ ), Lysine ( $\gamma\text{-H}$ ), Leucine ( $\beta, \gamma\text{-H}$ )
14	1.90	m	Arginine ( $\beta\text{-H}$ ), Lysine ( $\beta\text{-H}$ )
15	2.01	m	Proline ( $\gamma\text{-H}$ )
16	2.04	s	Glycoproteins lipid $\text{CH}_2\text{CH}=\text{CH}$
17	2.07	m	Prolone ( $\beta\text{-H}$ )
18	2.12	m	Glutamine ( $\beta\text{-H}$ )
19	2.14	s	Acetoacetate
20	2.27	m	Valine ( $\beta\text{-H}$ )
21	2.34	m	Prolone ( $\beta\text{-H}$ )
22	2.35	m	Glutamate ( $\gamma\text{-H}$ )
23	2.54	dd	Asparagine ( $\beta\text{-H}$ )
24	2.69	–	Asparagine ( $\beta\text{-H}$ ), Aspartic acid ( $\beta\text{-H}$ )
25	2.75	s	lipid $\text{CH}=\text{CHCH}_2\text{CH}=\text{CH}$
26	2.82	d	Aspartic acid ( $\beta\text{-H}$ )
27	3.03	t(7.7)	Lysine ( $\delta\text{-H}$ )
28	3.04	s	Creatinine
29	3.21	s	Choline
30	3.24	t(8)	Arginine ( $\delta\text{-H}$ )/Glucose
31	3.37	d(7)	Proline ( $\delta\text{-H}$ )
32	–	–	Glucose
33	3.54	m	Myo-inositol
34	3.58	d(8)	Threonine ( $\alpha\text{-H}$ )
35	3.62	d(7)	Valine ( $\alpha\text{-H}$ )
36	–	–	Glucose
37	3.77	d	Arginine ( $\alpha\text{-H}$ )
38	3.79	d	Lysine ( $\alpha\text{-H}$ )
39	3.91	–	Asparagine ( $\alpha\text{-H}$ ), Aspartic acid ( $\alpha\text{-H}$ )
40	4.08	brm	Myo-inositol
41	4.12	q	Lactate
42	4.13	–	Proline ( $\alpha\text{-H}$ )
43	4.25	m	Threonine ( $\alpha\text{-H}$ )
44	4.65	d(7)	$\beta\text{-Glucose}$ , H-1
45	5.19	br	Lipid, glyceryl
46	5.23	d(4)	$\alpha\text{-Glucose}$ , H-1
47	5.32	br	Lipid, $\text{CH}=\text{CH}$
48	6.89	d(8)	Tyrosine
49	7.18	d(8)	Tyrosine
50	7.32	d	Phenylalanine (ortho-)
51	7.37	t	Phenylalanine (para-)
52	7.43	dd	Phenylalanine (meta-)

peaks, which were obscured in the normal 1D spectrum (Fig. 2A), are observable following the relaxation editing, including those for amino acids (isoleucine  $\sim 1.01$  ppm, leucine  $\sim 0.97$  ppm, threonine  $\sim 1.32$  ppm, glutamate  $\sim 2.08/2.35$  ppm, glutamine  $\sim 2.12/2.44$  ppm, tyrosine  $\sim 6.89/7.18$  ppm), 3-hydroxybutyrate  $\sim 1.20$  ppm, and lactate at 4.12 ppm. For lipids, in addition to the usual alkyl peaks, the fatty acyl chains of lipids showed peaks at 2.75 and 5.32 ppm, indicating the presence of the structure  $-\text{CH}=\text{CH}-\text{CH}_2-\text{CH}=\text{CH}-$ .

All three relaxation filters are adjustable to discriminate against the broad protein and lipid peaks to various degrees to suit different purposes. Moreover, these three filters are extendable to 2D NMR spectroscopy to identify internuclear connectivity.

#### *T<sub>1</sub>/T<sub>1ρ</sub>/T<sub>2</sub>-edited COSY NMR spectroscopy of human blood plasma*

Fig. 3A shows the aliphatic region of a normal  $^1\text{H}$ - $^1\text{H}$  COSY spectrum of human blood plasma, in which most of the strong signals are readily observable such as these of lipids,  $\alpha$ - and  $\beta$ -glucose, and lactate. However, the weak peaks, such as those of proline (2.01/4.13, 2.34/4.13 ppm) and threonine (3.58/4.25 ppm), are not readily observable without large vertical expansions. In con-

trast, the  $T_1$ -,  $T_{1\rho}$ -, and  $T_2$ -edited COSY spectra (Figs. 3B–D) all showed great enhancement for the weak metabolite peaks, e.g., those of proline and threonine, as a consequence of the reduction of the lipid signals (e.g., 2.04/5.32, 2.75/5.32, and 1.29/0.89 ppm). The spectral editing clearly favored the detection of the small molecule metabolite signals. For example, following the relaxation editing, the signals of amino acids (valine, leucine, isoleucine) in the region at 0.7–2.0 ppm (dashed box in Figs. 3B–D) emerged much more clearly from under the intense lipid peaks. This provides an opportunity to resolve the overlapped signals in the regions of 1.20–1.33 and 0.80–1.05 ppm.

What is particularly encouraging is that the cross peaks for the  $\alpha$ -hydrogens of several amino acids are clearly displayed and can be assigned for arginine, alanine, valine, and threonine (Figs. 3B–D). They are normally overlapped with sugar signals and otherwise may be assigned only by “spiking.” Two observable cross peaks that were not readily observable without editing (Fig. 3A) are now also visible for proline (2.01/4.13, 2.34/4.13 ppm) and threonine (3.58/4.25 ppm) (Figs. 3B–D).

The advantage of this approach is illustrated even more clearly in the  $T_2$ -edited phase-sensitive DQF-COSY spectrum for human blood plasma (Fig. 4).

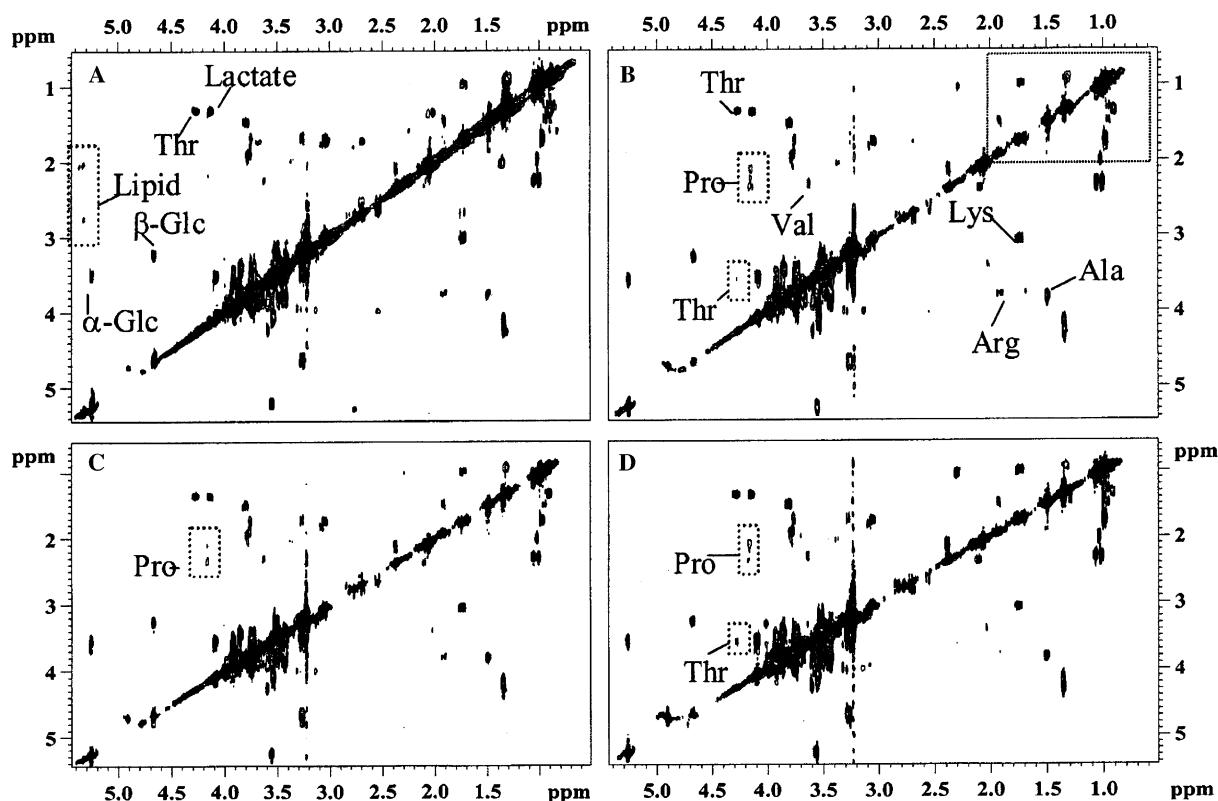


Fig. 3. Relaxation-edited  $^1\text{H}$ - $^1\text{H}$  COSY NMR spectra of human blood plasma recorded with the gradient selection and the recycle delay of 2 s. (A) Normal COSY spectrum; (B)  $T_1$ -edited spectrum;  $\tau_1 = 0.265$  s; (C)  $T_{1\rho}$ -edited spectrum; spin-locking power, 5 kHz; spin-locking time, 120 ms; (D)  $T_2$ -edited spectrum; relaxation delay, 400  $\mu\text{s}$ ; total loop, 400. 2K and 128 data points were acquired for f2 and f1 dimensions, respectively, and zero-filled to 2K by 2K before Fourier transformation.



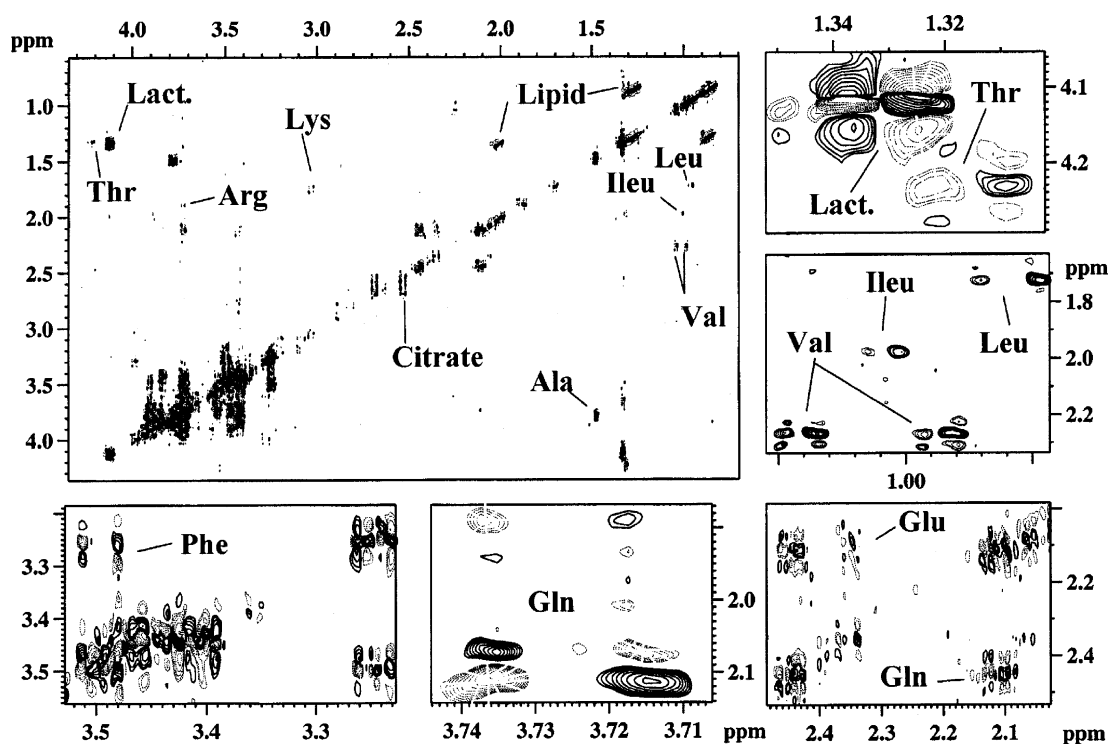


Fig. 4.  $T_2$ -edited phase-sensitive  $^1\text{H}$ - $^1\text{H}$  DQF-COSY NMR spectrum of human blood plasma recorded with the gradient selection and recycle delay of 2 s. In the  $T_2$  filter, the relaxation delay was 400  $\mu\text{s}$  and the total loop was 400. 2K and 128 data points were acquired for f2 and f1 dimensions, respectively, and zero-filled to 2K by 2K before Fourier transformation. Phase increment in f1 was carried out with TPPI. Thick solid and faint dashed lines indicate the positive and negative contours.

Resolved peaks for amino acids, such as glutamine, glutamate, threonine, leucine, and isoleucine, were detectable more readily than in the unedited spectrum (data not shown). With the excellent resolution in this spectrum, the unambiguously resolved signals for threonine and lactate are observed in the expanded region at 1.31–1.35/4.0–4.35 ppm since the lipid  $\text{CH}_2$  signals are substantially attenuated with  $T_2$ -editing. In this experiment, the flip-back pulse (p1 in Fig. 1G) leads to independence for the phase cycles of the relaxation editing and that of the 2D NMR, making implementation of the phase-sensitive 2D NMR feasible.

#### $T_1/T_{1\rho}/T_2$ -edited TOCSY NMR spectroscopy of human blood plasma

Fig. 5A shows a normal  $^1\text{H}$ - $^1\text{H}$  TOCSY NMR spectrum of control human blood plasma, in which the lipid peaks (0.89/1.29, 1.29–2.04–2.7–5.32 ppm) are dominating. Consequently, it is much harder to observe the less intense peaks close to the lipid signals, such as isoleucine (0.94/1.27, 0.94/1.46, 1.01/1.27, and 1.01/1.46 ppm), leucine (0.97/1.72 ppm), threonine (3.58/4.25 ppm), and proline (4.13/2.01, 2.34/4.13 ppm). However, the  $T_1$ -edited 2D TOCSY spectrum (Fig. 5B) clearly shows drastic reduction of the lipid signal in-

tensity relative to the signals of the amino acids. As a result, the peaks of proline (4.13/2.01, 4.13/2.34 ppm) and threonine (4.25/3.58 ppm) are detectable with their proton connectivity. Peaks for aspartate and asparagine are better resolved and the region at 0.9–2.0 ppm (in the dotted box) also showed much improved resolution for isoleucine and leucine.

In theory, the  $T_{1\rho}$ -edited TOCSY spectrum can be implemented with a relaxation preparation followed with 2D as shown in Fig. 1E and by simply using a long mixing time, during which  $T_{1\rho}$  relaxation will take place at the field strength of the TOCSY spin-lock field. Clearly, the second approach is restricted by the choice of TOCSY parameters (mixing time and spin-lock field strength). Fig. 5C shows a spectrum obtained from the second approach using an MLEV-17 spin-locking scheme. It is clear that, compared to the normal TOCSY spectrum (Fig. 5A), the  $T_{1\rho}$ -edited TOCSY spectrum (Fig. 5C) showed some signal attenuation for the lipids and hence enhancement of the sharp peaks of the small metabolites. However, the attenuation of lipid peaks is observed to be of a lesser extent (compared that of to  $T_1$ - and  $T_2$ -editing). This is due to the restriction on the spin-lock parameters to satisfy the need of TOCSY sequence. The method described in Fig. 1E, nevertheless, will not suffer from this restriction because the spin-

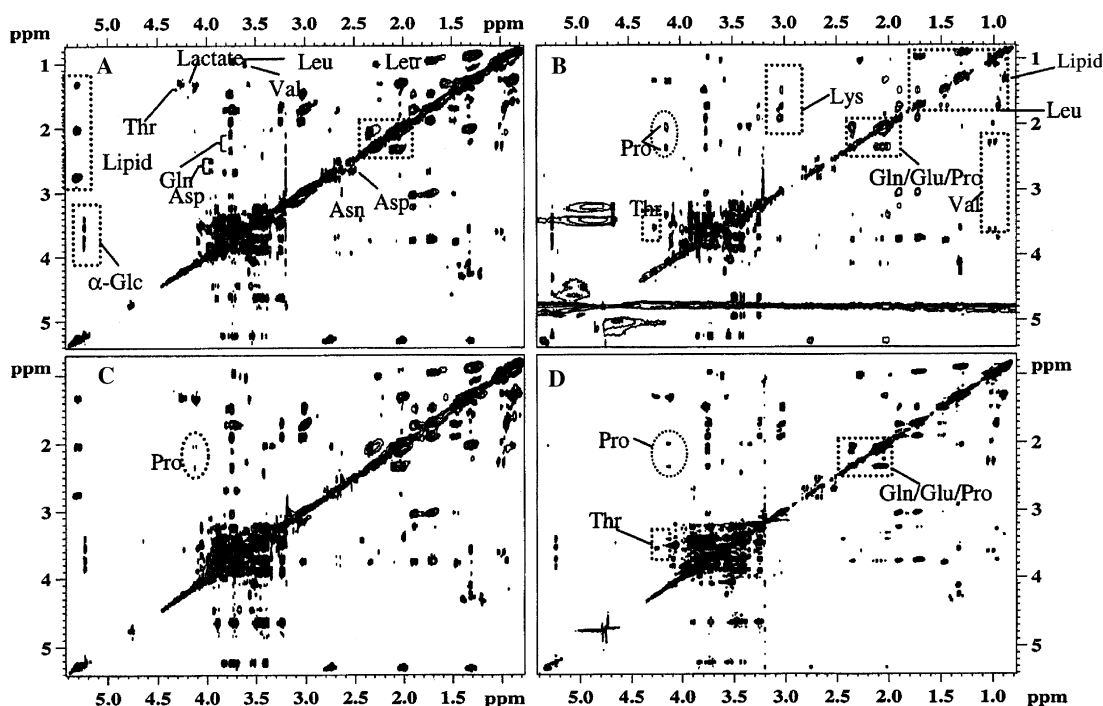


Fig. 5. Relaxation-edited  $^1\text{H}$ - $^1\text{H}$  TOCSY NMR spectra of human blood plasma recorded using MLEV17 as spin-locking scheme and WATERGATE sequence [37] as solvent suppression scheme. TPPI was used for the phase incrementation in f1. The mixing time was 90 ms with exception in the  $T_{1\rho}$ -edited spectrum; the recycle delay was 2 s. (A) Normal TOCSY spectrum; (B)  $T_1$ -edited spectrum;  $\tau_1 = 0.265$  s; (C)  $T_{1\rho}$ -edited spectrum; spin-locking power, 5 kHz; spin-locking time, 120 ms as mixing scheme; (D)  $T_2$ -edited spectrum, relaxation delay, 400  $\mu\text{s}$ ; total loop, 250. 2K and 128 data points were acquired for f2 and f1 dimensions, respectively, and zero-filled to 2K by 2K before Fourier transformation.

locking power for  $T_{1\rho}$  becomes independent from the TOCSY mixing pulses and it thus can be adjusted to a much lower power level.

A  $T_2$ -edited TOCSY NMR spectrum recorded with the sequence illustrated in Fig. 1E is shown in Fig. 5D with a total  $T_2$  relaxation duration ( $2n\tau_E$ ) of 200 ms. The strategy in general is the same as that employed previously [26]. However, a flip-back pulse was employed immediately after the CPMG preparation to facilitate easy phase incrementation in the second dimension of the 2D experiment. Cross peaks are now readily observable for amino acids such as valine, alanine, glutamine, glutamate, lysine, arginine, leucine, and isoleucine, sugars such as  $\alpha$ -glucose and  $\beta$ -glucose, and hydroxycarboxylates, such as citrate and 3-hydroxybutyrate, which are hardly visible in the 1D NMR spectrum. The cross peaks at 2.12/3.72 for glutamine and 1.01/1.27, 1.01/1.46 ppm for isoleucine which are not detectable in the unedited TOCSY or 1D NMR are also observable. It is particularly encouraging to note that cross peaks help to unambiguously assign threonine peaks overshadowed by the lactate and lipid peaks. A  $T_2$ -edited TOCSY spectrum of this human blood plasma sample with a much longer relaxation delay ( $2n\tau_E$ ) of 400 ms is also displayed in Fig. 6, showing that the method is robust. In this spectrum, the cross peaks observed at 0.89/1.29, 1.29-2.04-2.75-5.32 ppm (data not shown) are consistent with the fatty acyl structure hav-

ing a fragment as expected of  $\text{CH}_3(\text{CH}_2)_4\text{CH}=\text{CH}-\text{CH}_2-\text{CH}=\text{CH}$ . An expansion of the regions 2.0–2.9 ppm (upper left inset) showed excellent resolution for aspartic acid, asparagine, glutamic acid, glutamine, and proline, which are not readily achievable with the normal TOCSY. The connectivity of aromatic protons is also clearly displayed for tyrosine and phenylalanine (lower left inset). The overall quality of the edited TOCSY spectrum is improved compared to those reported previously for plasma [26].

This experiment is particularly useful to enable the detection of some possible metabolites buried under big broad peaks. For example, in the literature, there has been debate about detection of fucose in blood plasma [42,43] of a cancer patient. Although this sugar was not detected in this sample (a control sample), the experiments described here should be useful to detect such chemical moieties since the cross peaks should be detected between the methyl group (1.32), the H-5 (4.13), and the rest of the ring protons for fucose.

#### $T_2$ -edited J-resolved 2D NMR spectroscopy

A  $T_2$ -edited J-resolved 2D NMR method where the experiment was employed to eliminate water signals and to characterize solutes has already been reported [24]. However, no applications of this approach for blood plasma or tissues have been reported so far. In effect, the

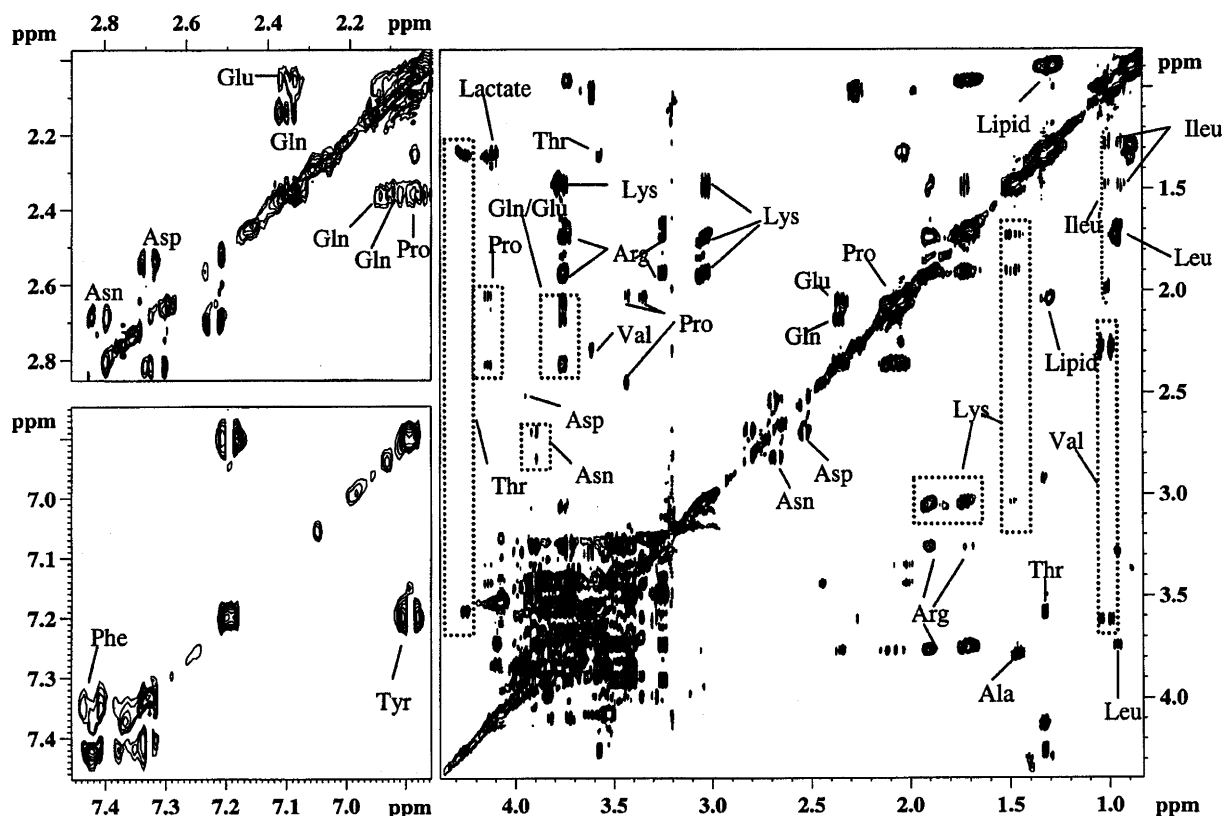


Fig. 6.  $T_2$ -edited  $^1\text{H}$ - $^1\text{H}$  TOCSY NMR spectra of human blood plasma recorded using MLEV17 as spin-locking scheme and TPPI for the phase incrementation in  $f_1$ . The mixing time was 90 ms and recycle delay was 2 s. The relaxation delay was 400  $\mu\text{s}$  and the total loop was 512. 2K and 128 data points were acquired for  $f_2$  and  $f_1$  dimensions, respectively, and zero-filled to 2K by 2K before Fourier transformation.

J-resolved 2D NMR is a  $T_2$ -edited experiment itself. However, the extent of such editing is dependent on the spectral width and the total increment time in the second dimension ( $f_1$ ). For a normal J-resolved experiment with 48 increments and spectral width of 50 Hz in  $f_1$  (digital resolution of 1.04 Hz), the first increment time (spin-echo delay) will be about 20 ms, which is too short to edit out the broad signals substantially (requiring  $>200$  ms). Therefore, some broad peaks could still be present in the spectrum. If a true  $T_2$  filter is inserted prior to the J-resolved sequence, the  $T_2$ -editing process is completely controlled. A  $T_2$ -edited J-resolved NMR spectrum of human blood plasma (Fig. 7) gives direct information on the multiplicity structure of the observed signals and provides confirmation of the observations in the previous NMR spectra. The  $T_2$ -edited phase-sensitive DQF-COSY spectrum should provide similar information in many cases in addition to connectivity information. As in the normal 2D NMR, the  $T_2$ -edited experiments are particularly useful for the detection and assignment of the low-concentration metabolites in complex biofluids. Although only the  $T_2$ -edited J-resolved experiment has been demonstrated here, the  $T_1$ - and  $T_{1\rho}$ -edited versions can be implemented in a similar fashion.

## Conclusion

Relaxation-edited 1D and 2D NMR spectroscopy is a powerful method to detect NMR peaks for the small molecules masked by intense and broad resonances in multiphase, multicompartiment biological samples. For 2D NMR experiments, the introduction of a flip-back pulse prior to 2D sequences makes the phase cycling for the relaxation filters independent from the 2D parts, thus making it easy to implement phase-sensitive 2D NMR experiments. In addition, these methods enable higher receiver gains to be employed, offering greater dynamic range for detection and assignment of low-concentration metabolites in biological samples or low-concentration molecules in other heterogeneous systems. All three relaxation times,  $T_1$ ,  $T_{1\rho}$ , and  $T_2$  can be easily employed to edit the complex 1D and 2D NMR spectra. For blood plasma samples, the  $T_1$ -,  $T_{1\rho}$ -, and  $T_2$ -based editing methods are all efficient to edit out protein/lipoprotein signals by choosing appropriate "relaxation filters." The  $T_1$ -editing enables one to selectively detect metabolites by using an appropriate relaxation delay ( $\tau_1 \sim \ln 2 \cdot T_1$  of proteins/lipoproteins) or proteins/lipoproteins ( $\tau_1 < \ln 2 \cdot T_1$  of metabolites) or metabolites as negative peaks and proteins/lipoproteins as positive

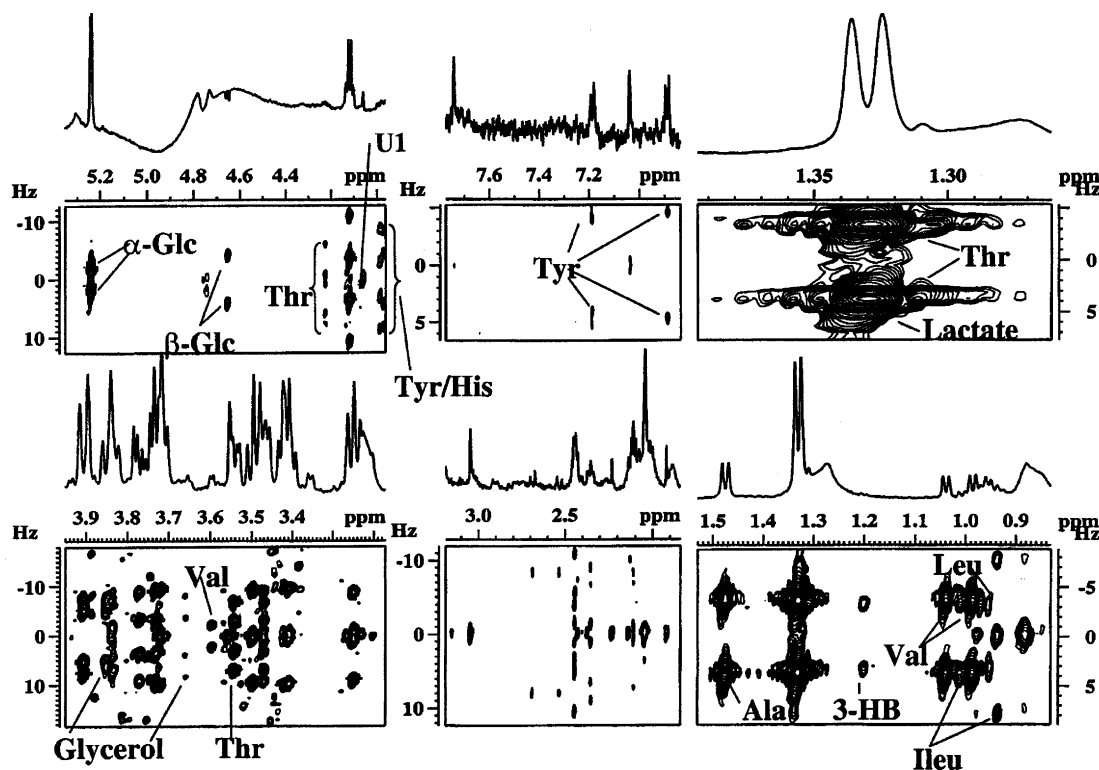


Fig. 7.  $T_2$ -edited  $^1\text{H}$ - $^1\text{H}$  J-resolved NMR spectrum of human blood plasma recorded with the recycle delay of 2 s. In the  $T_2$  filter, the relaxation delay was  $400\ \mu\text{s}$  and the total loop was 400. 2K and 48 data points were acquired for  $f_2$  and  $f_1$  dimensions, respectively. The spectrum was “tilted” after Fourier transformation. U1 is an unassigned resonance.

peaks in the same spectrum ( $\text{Ln}2 \cdot T_1$  of proteins/lipoproteins  $< \tau_1 < \text{Ln}2 \cdot T_1$  of metabolites). Apart from  $T_1$ -editing, diffusion editing is the only other technique that one can employ to detect proteins/lipoproteins without metabolites signals. The choice of an editing method is dependent on the sample systems and the differences between the relaxation times of metabolites and proteins/lipoproteins. For biological tissues, with optimized parameters, these editing methods are expected to be equally useful. However, for urine samples, they are less useful to detect metabolites since most of the signals of urine samples are from small metabolites. It may be useful to detect macromolecules there and both  $T_1$ - and diffusion-editing techniques are expected to be effective. The relaxation-edited approaches can be used easily in most other types of 2D NMR spectroscopy, such as ROESY, and the inverse-detected 2D experiments, such as HSQC, in a similar fashion and this line of work is ongoing. Although demonstrated with a blood plasma sample, the catalogue of techniques is expected to be useful in combinatorial chemistry also.

#### Acknowledgments

Drs. Mary Bollard and Bridgette Beckwith-Hall (Imperial College) are acknowledged for their advice in sample preparation. We also acknowledge some anon-

ymous referees for their suggestions and constructive criticism, which helped to improve the manuscript.

#### References

- [1] J.K. Nicholson, I.D. Wilson, High-resolution proton magnetic-resonance spectroscopy of biological fluids, *Prog. NMR Spectrosc.* 21 (1989) 449–501.
- [2] J.K. Nicholson, M.J. Buckingham, P.J. Sadler, High-resolution  $^1\text{H}$  NMR studies of vertebrate blood and plasma, *Biochem. J.* 211 (1983) 605–615.
- [3] J.K. Nicholson, M.P. Offlynn, P.J. Sadler, A.F. MacLeod, S.M. Juul, P.H. Sonksen, Proton nuclear-magnetic-resonance studies of serum, plasma and urine from fasting normal and diabetic subjects, *Biochem. J.* 217 (1984) 365–375.
- [4] J.K. Nicholson, P.J.D. Foxall, M. Spraul, R.D. Farrant, J.C. Lindon, 750-MHz  $^1\text{H}$  and  $^1\text{H}$ - $^{13}\text{C}$  NMR-spectroscopy of human blood-plasma, *Anal. Chem.* 67 (1995) 793–811.
- [5] P.J.D. Foxall, J.A. Parkinson, I.H. Sadler, J.C. Lindon, J.K. Nicholson, Analysis of biological-fluids using 600 MHz proton NMR-spectroscopy-application of homonuclear 2-dimensional J-resolved spectroscopy to urine and blood plasma sterling for spectral simplification and assignment, *J. Pharm. Biomed. Anal.* 11 (1993) 21–31.
- [6] R.A. Wevers, U. Engelke, A. Heerschap, High resolution  $^1\text{H}$ -NMR spectroscopy of blood plasma for metabolic studies, *Clin. Chem.* 40 (1994) 1245–1250.
- [7] Y.L. Wang, M.E. Bollard, H. Keun, H. Antti, O. Beckonert, T. Ebbels, J.C. Lindon, E. Holmes, H.R. Tang, J.K. Nicholson, Spectral Editing and pattern recognition methods applied to

- high-resolution magic-angle-spinning  $^1\text{H}$  NMR spectroscopy of liver tissues, *Anal. Biochem.* 323 (2003) 26–32.
- [8] M.L. Liu, J.K. Nicholson, J.C. London, High-resolution diffusion and relaxation edited one- and two-dimensional  $^1\text{H}$  NMR spectroscopy of biological fluids, *Anal. Chem.* 68 (1996) 3370–3376.
- [9] D.H. Wu, A.D. Chen, C.S. Johnson, An improved diffusion-ordered spectroscopy experiment incorporating bipolar-gradient pulses, *J. Magn. Reson. A* 115 (1995) 260–264.
- [10] M.L. Liu, J.K. Nicholson, J.A. Parkinson, J.C. Lindon, Measurement of biomolecular diffusion coefficients in blood plasma using two-dimensional  $^1\text{H}$ - $^1\text{H}$  diffusion-edited total-correlation NMR spectroscopy, *Anal. Chem.* 69 (1997) 1504–1509.
- [11] M.L. Liu, H.R. Tang, J.K. Nicholson, J.C. Lindon, Use of  $^1\text{H}$  NMR determined diffusion coefficients to characterize lipoprotein fractions in human blood plasma, *Magn. Reson. Chem.* (2002) S83–S88.
- [12] E.K. Gozansky, D.G. Gorenstein, DOSY-NOESY: diffusion-ordered NOESY, *J. Magn. Reson. B* 111 (1996) 94–96.
- [13] D.H. Wu, A.D. Chen, C.S. Johnson, Three-dimensional diffusion-ordered NMR spectroscopy: the homonuclear COSY-DOSY experiment, *J. Magn. Reson. A* 121 (1996) 88–91.
- [14] H.R. Tang, Y.L. Wang, P.S. Belton,  $^{13}\text{C}$  CPMAS studies of plant cell wall materials and model systems using proton relaxation-induced spectral editing techniques, *Solid State NMR* 15 (2000) 239–248.
- [15] H.R. Tang, B.P. Hills, in: G.A. Webb, P.S. Belton, A.M. Gil, I. Delgadillo (Eds.), *Magnetic Resonance in Food Science—A View to the Future*, Royal Society of Chemistry, Cambridge, 2001, pp. 155–164.
- [16] K. Schmidtrohr, J. Clauss, H.W. Spiess, Correlation of structure, mobility, and morphological information in heterogeneous polymer materials by 2-dimensional wideline-separation nmr-spectroscopy, *Macromolecules* 25 (1992) 3273–3277.
- [17] N. Zumbulyadis, Selective carbon excitation and the detection of spatial heterogeneity in cross-polarization magic-angle-spinning NMR, *J. Magn. Reson.* 53 (1983) 486–494.
- [18] H.R. Tang, B.P. Hills, Use of  $^{13}\text{C}$  MAS NMR to study domain structure and dynamics of polysaccharides in the native starch granules, *Biomacromolecules* 4 (2003) 1269–1276.
- [19] R.H. Newman, L.M. Davies, P.J. Harris, Solid-state C-13 nuclear magnetic resonance characterization of cellulose in the cell walls of *Arabidopsis thaliana* leaves, *Plant Physiol.* 111 (1996) 475–485.
- [20] F.W. Benz, J. Feeney, G.C.K. Roberts, Fourier transform proton NMR spectroscopy in aqueous solution, *J. Magn. Reson.* 8 (1972) 114–121.
- [21] D.L. Rabenstein, S. Fan, T.T. Nakashima, Attenuation of the water resonance in fourier-transform  $^1\text{H}$ -Nmr spectra of aqueous-solutions by spin-spin relaxation, *J. Magn. Reson.* 64 (1985) 541–546.
- [22] P.G. Williams, J.K. Saunders, M. Dyne, C.E. Mountford, K.T. Holmes, Application of  $T_2$ -filtered COSY experiment to identify the origin of slowly relaxing species in normal and malignant tissue, *Magn. Reson. Med.* 7 (1988) 463–471.
- [23] J.K. Saunders, J.D. Stevens, Application of partially relaxed 2D-COSY spectra in special assignments of carbohydrates, *Magn. Reson. Chem.* 24 (1986) 1023–1025.
- [24] D.L. Rabenstein, G.S. Srivatsa, R.W.K. Lee, Two-dimensional J-resolved  $^1\text{H}$ -NMR spectra of aqueous-solutions with complete elimination of the water resonance, *J. Magn. Reson.* 71 (1987) 175–179.
- [25] D.L. Rabenstein, K.K. Millis, E.J. Strauss, Proton NMR spectroscopy of human blood plasma, *Anal. Chem.* 60 (1988) 1380A–1391A.
- [26] D. Trehout, M. Desille, B.T. Doan, S. Mahler, B. Fremont, Y. Malledant, J.P. Campion, J. Desbois, J.C. Beloeil, J. Certaines, B. Clement, Follow-up by one- and two-dimensional NMR of plasma from pigs with ischemia-induced acute liver failure treated with a bioartificial liver, *NMR Biomed.* 15 (2002) 393–403.
- [27] S. Meiboom, D. Gill, Modified spin-echo method for measuring nuclear relaxation times, *Rev. Sci. Instrum.* 29 (1958) 688–691.
- [28] M. Vonkienlin, C.T.W. Moonen, A. Vandertoorn, P.C.M. Van-zijl, Rapid recording of solvent-suppressed 2D COSY spectra with inherent quadrature detection using pulsed field gradients, *J. Magn. Reson.* 93 (1991) 423–429.
- [29] D. Neuhaus, I.M. Ismail, C.W. Chung, “FLIPSY”—A new solvent-suppression sequence for nonexchanging solutes offering improved integral accuracy relative to 1D NOESY, *J. Magn. Reson. A* 118 (1996) 256–263.
- [30] Y.L. Wang, P.S. Belton, H.R. Tang, Proton NMR relaxation studies of solid L-alaninamide, *Chem. Phys. Lett.* 268 (1997) 387–392.
- [31] P. Belton, Y.L. Wang, Proton NMR relaxation studies of solid L-leucinamide, *Mol. Phys.* 90 (1997) 119–125.
- [32] H.R. Tang, P.S. Belton, Molecular motions of D-alpha-galacturonic acid (GA) and methyl-D-alpha-galacturonic acid methyl ester (MGAM) in the solid state—a proton NMR study, *Solid State NMR* 12 (1998) 21–30.
- [33] Y.L. Wang, P.S. Belton, H.R. Tang, Proton NMR relaxation studies of solid tyrosine derivatives and their mixtures with L-leucinamide, *Solid State NMR* 14 (1999) 19–32.
- [34] Y.L. Wang, H.R. Tang, P.S. Belton, Solid state NMR studies of the molecular motions in the polycrystalline  $\alpha$ -L-fucopyranose and methyl  $\alpha$ -L-fucopyranoside, *J. Phys. Chem. B* 106 (2002) 12834–12840.
- [35] H.R. Tang, P.S. Belton, Molecular dynamics of polycrystalline cellobiose studied by solid state NMR, *Solid State NMR* 21 (2002) 117–133.
- [36] S. Braun, H.O. Kalinowski, S. Berger, 150 and More Basic NMR Experiments, A Practical Course, Wiley-VCH, Chichester, 1998.
- [37] M.L. Liu, X.A. Mao, C.H. Ye, H. Huang, J.K. Nicholson, J.C. Lindon, Improved WATERGATE pulse sequences for solvent suppression in NMR spectroscopy, *J. Magn. Reson.* 132 (1998) 125–129.
- [38] A.E. Derome, *Modern NMR Techniques for Chemistry Research*, Oxford University Press, Oxford, 1987.
- [39] A. Bax, D.G. Davis, MLEV-17-based two-dimensional homonuclear magnetisation transfer spectroscopy, *J. Magn. Reson.* 65 (1985) 355–360.
- [40] S.P. Rucker, A.J. Shaka, Broadband homonuclear cross polarization in 2D NMR using DIPSI2, *Mol. Phys.* 68 (1989) 509–517.
- [41] R.K. Harris, *Nuclear Magnetic Resonance Spectroscopy*, Pitman Books, London, 1983.
- [42] P.S. Phillips, F.G. Herring, Is the detection of fucose cancer markers by 2D  $^1\text{H}$  NMR unequivocal? *Magn. Reson. Med.* 15 (1990) 1–7.
- [43] C.E. Mountford, Detection of malignant-tumours by nuclear-magnetic-resonance spectroscopy of plasma, *N. Eng. J. Med.* 316 (1987) 1414–1415.